Original article

Determining how the pattern of bone healing affects the strain of plate implant via frequency detection: a biomechanical cadaveric study

Chavarin Amarase[a, b, c], **Chanyaphan Virulsri**[d, e, f, *], **Pairat Tangpornprasert**[d, e, f], **Pisitpong Chancharoen**[d, e], **Saran Tantavisut**[b, c]

[a]*Biologics for Knee Osteoarthritis Research Unit, Faculty of Medicine, Chulalongkorn University, Bangkok, Thailand*
[b]*Center of Excellence in Hip Fracture, Department of Orthopaedics, Faculty of Medicine, Chulalongkorn University, Bangkok, Thailand*
[c]*Department of Orthopaedics, Faculty of Medicine, Chulalongkorn University, Bangkok, Thailand*
[d]*Center of Excellence for Prosthetic and Orthopedic Implant, Chulalongkorn University, Bangkok, Thailand*
[e]*Biomedical Engineering Research Center, Faculty of Engineering, Chulalongkorn University, Bangkok, Thailand*
[f]*Department of Mechanical Engineering, Faculty of Engineering, Chulalongkorn University, Bangkok, Thailand*

Abstract

Background: Detecting bone union is crucial in treating bone fractures to prevent complications, including implant failure and bone nonunion. To date, there are numerous methods and new innovative devices for detecting bone union via strain measurements, such as strain gauges, fluid level displacement, contrast media, and frequency changes. Moreover, there is a trend toward increasing these methods in the future. However, the patterns of bone healing studied with these methods do not provide a standard for determining the true bone healing process.

Objective: This study aimed to identify the most appropriate bone healing pattern for detecting bone healing using strain measurements via frequency changes.

Methods: Twenty cadaveric tibial bones were tested for five different bone healing patterns, including fractures with gap distances, material replacements, and healing from the outer side, inner side, and middle. Each healing pattern included four cadaveric bones evaluated under various axial loads of 100, 200, 300, and 400 N using an Instron ElectroPuls® E10000. Bone healing assessment employed bone union detection using a wire's natural frequency plate to detect the strain change via frequency change.

Results: All bone healing patterns could evaluate bone union by comparing the frequency changes under axial loads of 100 and 400 N, with a mean difference of 32.4–39.8%. Only the fracture with gap distance and material replacement could be assessed gradually in each phase of healing (12.3% in gap of 2.5 mm, $P < 0.01$; 22.4% in gap of 5 mm, $P = 0.04$; 31.8% in gap of 7.5 mm, $P = 0.005$; 39.2% in gap of 10 mm, $P = 0.004$; and 11.0% in saw bone, $P = 0.006$; 19.5% in rubber, $P < 0.001$; 25.8% in foam, $P < 0.001$; 32.4% in fracture, $P < 0.001$).

Conclusions: The pattern of bone healing influences the assessment of bone union via the detection of strain changes. The methods involving gap distance and material replacement are the most suitable representation of normal bone healing.

Keywords: Acoustic, bone healing, frequency, pattern, plate, strain, union.

***Correspondence to: Chayaporn Hasdiseve,** Center of Excellence for Prosthetic and Orthopedic Implant, Chulalongkorn University, Bangkok 10330, Thailand.
E- mail: Chanyaphan.v@eng.chula.ac.th
Received: September 11, 2025
Revised: December 12, 2025
Accepted: January 20, 2026

Bone fractures are among the most common orthopedic conditions.[1-4] Treatment methods include conservative approaches and surgical fixation, the aim of which is to achieve bone union. Complications, such as nonunion and implant failure, can be prevented if surgeons detect these issues early and initiate timely treatment.[5] Assessing bone healing is vital during the fracture treatment process.[6, 7] Most orthopedic surgeons rely on history taking, physical examinations, and plain radiographs to evaluate bone healing. However, there are various other methods available to assist in this assessment,[8, 9] including ultrasound,[10] computed tomography scans (CT scans),[11, 12] magnetic resonance imaging (MRI),[13, 14] nuclear imaging,[15] and innovative devices designed to detect strain changes.[16-25]

The concept of assessing bone healing through detecting changes in strain is illustrated in **Figure 1.** When a bone fractures and immediate fixation occurs, the strain at the center of the plate in the fracture area is at its maximum during axial loading. As bone healing progresses, the strain on the plate decreases until bone union occurs, at which point it is at its minimum. This suggests that if orthopedic surgeons can detect changes in the strain of the device, they can predict the bone healing status.

Many innovative devices have been developed in the past two decades. Most of them employ strain changes to assess bone healing via various methods such as strain gauges,[16] changes in resonance response frequency (RRF),[17] wavelength,[18] piezoelectric voltage,[19] telemetry values,[20] tungsten displacement,[21] contrast media,[22] fluid levels,[23] force sensor,[24] and the frequency of wire in bone union detection using a wire's natural frequency (BUDWF) plate.[25] The experiments for these innovations were conducted on humans,[20] animals,[16, 17] cadaveric bone,[22, 25] and sawbones[18, 19, 21, 24] with various bone healing patterns, including fractures with gap distances,[16-18, 21, 22, 25] material replacements,[19, 24] and healing from different sites.

However, the standard for bone healing patterns required for experiments in these studies has not been established. This study aimed to define the most suitable bone healing pattern for detecting healing through strain measurement. The method utilized in this study to detect changes in strain is the frequency change with the BUDWF plate.[25]

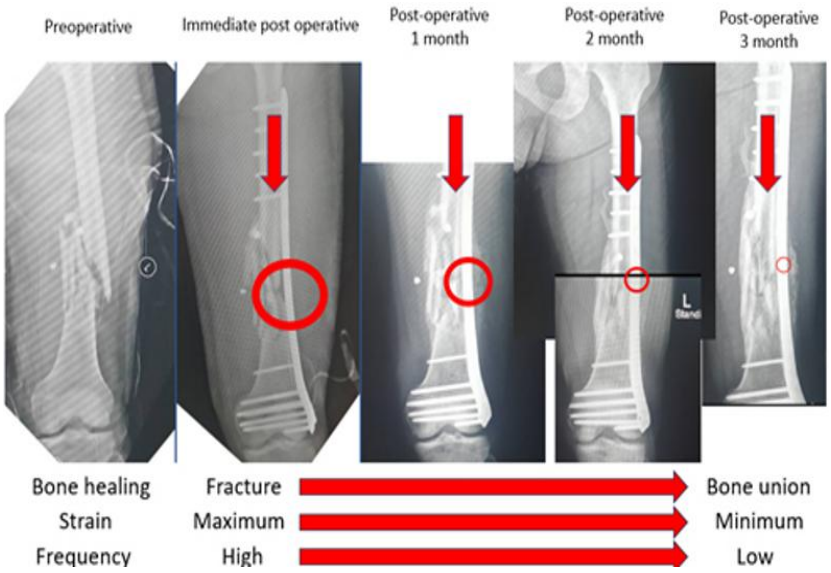

Figure 1. The concept of assessing bone healing through detecting changes in strain.

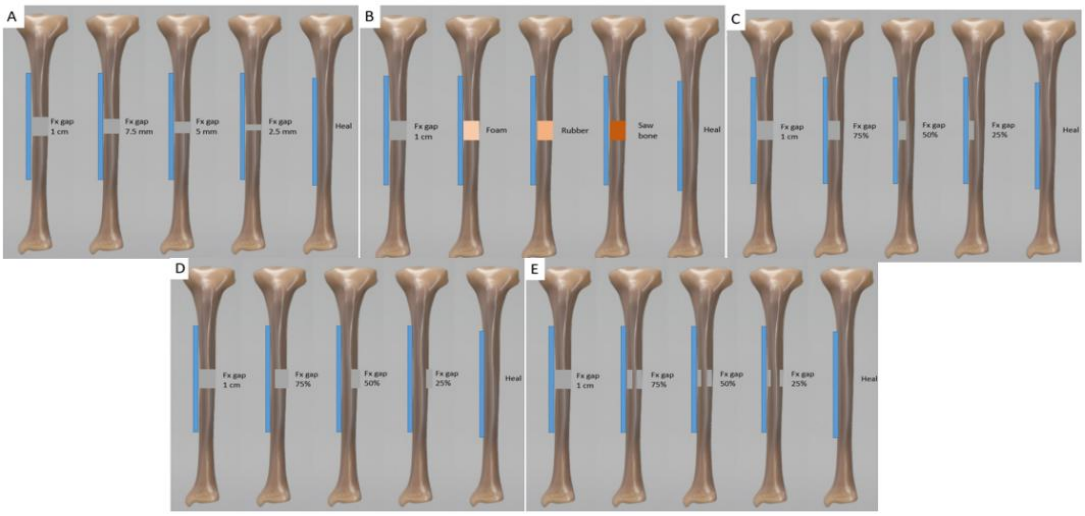

Figure 2. Images of the five bone healing patterns, each with five stages: **(A)** gap distances (gap of 10 mm, 7.5 mm, 5 mm, 2.5 mm, and healing); **(B)** material replacement (fracture, foam, rubber, sawbone, and healing); **(C)** healing from the outer side (fracture, 25.0% healing, 50.0% healing, 75.0% healing, and complete healing); **(D)** healing from the inner side (fracture, 25.0% healing, 50.0% healing, 75.0% healing, and complete healing); **(E)** healing from the middle (fracture, 25.0% healing, 50.0% healing, 75.0% healing, and complete healing).

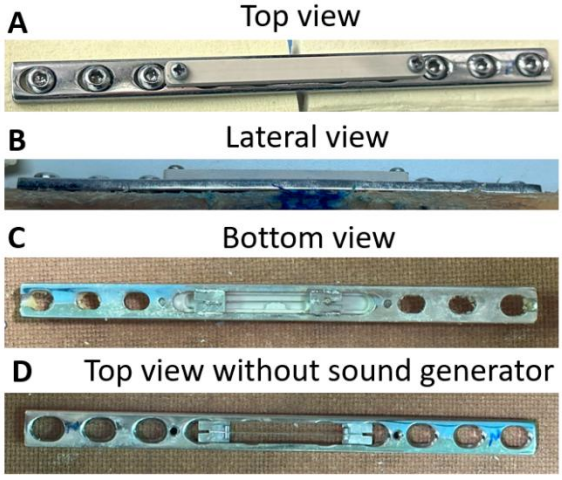

Figure 3. Images of the bone healing assessment utilizes bone union detection using a wire's natural frequency (BUDWF) plate: **(A)** top view; **(B)** lateral view; **(C)** bottom view; **(D)** top view without sound generator.

Materials and methods

Twenty cadaveric tibial bones were tested in this study. We defined the bone healing pattern as consisting of five patterns, namely 1) gap distance; 2) material replacement; 3) healing from the outer side; 4) healing from the inner side; and 5) healing from the middle. Each bone healing pattern was subclassified into five stages to represent the gradual process of bone healing; for example, the gap distance pattern included stages for the fracture gap of 10, 7.5, 5, and 2.5 mm, and the healing stage, as shown in **Figure 2**. Each bone healing pattern was tested using four cadaveric tibial bones under various axial loads of 100, 200, 300, and 400 N with an Instron ElectroPuls® E10000. In addition, we used the Bone Healing Assessment, which employs the BUDWF plate[25] to detect changes in strain.

Bone healing assessment utilizes the BUDWF plate[25]

The BUDWF plate was modified from a narrow dynamic compression plate with 10 holes (dimension of 167 × 12 × 4 mm, made from 316L stainless steel). The middle four holes were cut to create a slot. A 316L stainless steel wire with a diameter of 0.3 mm and a length of 40 mm was attached along the middle of the slot using a laser welding technique. The wire was set to a frequency of 2000–3500 Hz to avoid environmental noise. The sound generator was made from polyetheretherketone (PEEK) and had a pointed edge at the bottom that could strike the wire to produce noise when the top of the sound generator was pressed. The sound generator was attached to the plate with two screws. The BUDWF plate is shown in **Figure 3**.

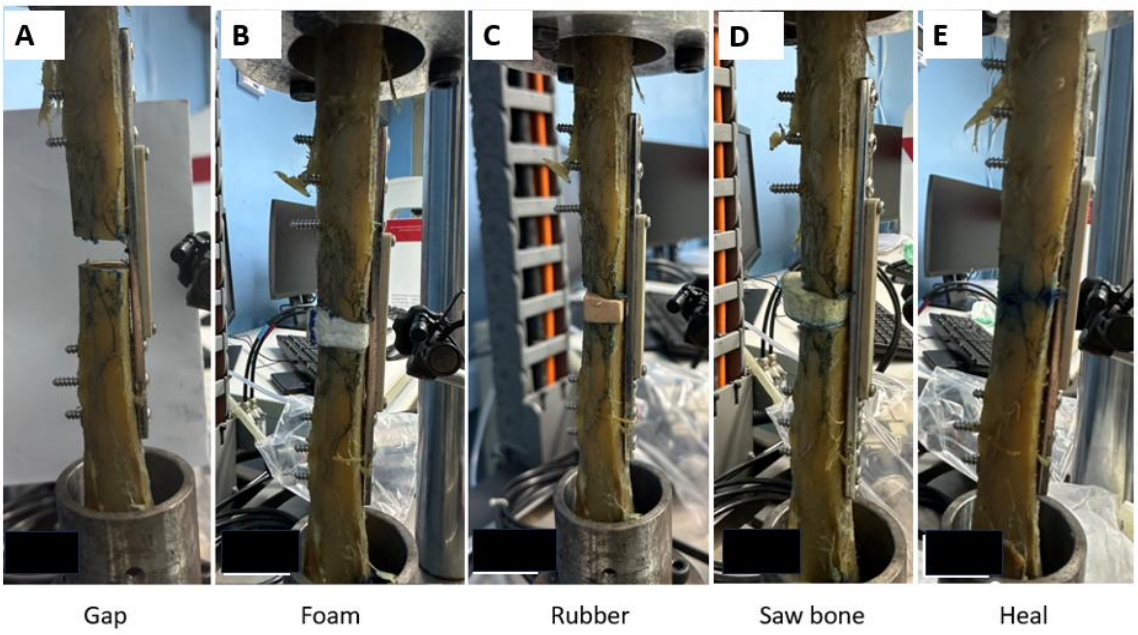

Figure 4. Images of the experimental setup for bone healing patterns resulting from material replacement across five stages: **(A)** fracture; **(B)** foam; **(C)** rubber; **(D)** sawbone; and **(E)** heal.

The concept of the BUDWF plate is that it can detect changes in strain as well as changes in frequency, as shown in **Figure 1**. When a fracture is treated with immediate fixation, the strain is highest when axial load is applied, and the tension in the wire also reaches its peak, thereby resulting in a high frequency. As the bone heals, the strain on the plate's frequency gradually decreases, with a corresponding decrease in the frequency of the wire until bone union occurs. At this point, the strain on the plate is minimal, and the wire's frequency is at its lowest. Therefore, if a change in frequency is detected, it indicates a change in the strain and bone healing.

Experimental setup

Cadaveric tibial bone was cut from the proximal to the distal shaft. The tibia was placed into the Instron ElectroPuls® E10000 (a machine for dynamic and static material tests that can determine the axial load, time to load, duration, interval, and cycle). A Synco G1A1 condenser microphone was positioned approximately 2 cm from the center of sound generation on the plate. Sound was analyzed using the Audacity program to measure the frequency. The experimental setup is illustrated in **Figure 4**, depicting the bone healing pattern with material replacement.

In the gap distance, healing from the outer side, inner side, and middle, tests began with the healing stage (uncut bone) under various axial loads of 100, 200, 300, and 400 N, applied at a rate of 10 N/s. Following this, the same test was performed on healing at 25.0%, 50.0%, 75.0%, and the fracture stage. The bone diameter was measured, and the bone was cut in stages at 1 cm intervals. First, 25.0% of the diameter was removed (bone healing 75.0%), then 50.0% (bone healing 50.0%), then 75.0% (bone healing 25.0%), and finally, all remaining bone was cut (bone fracture). The cuts were made starting from a direction that depended on the bone healing pattern group. Moreover, in the material replacement pattern, the test started with the healing stage. Next, the tibial bone was cut with a fracture gap of 10 mm and inserted with material that gradually increased the elastic modulus. In this study, foam, rubber, and sawbone were used to represent the bone healing process.[19, 26] For each loading force, sound was produced 10 times and recorded using a microphone. The mean frequency was analyzed using the Audacity program.

After receiving approval from the university's Institutional Review Board (IRB No. 0395/65, COE No. 026/2022), four cadaveric tibial bones were tested for each bone healing pattern. Each stage of the bone healing pattern was examined using the same technique described in the experimental setup.

Statistical analysis

The frequency of the wire was expressed as the mean value. The frequency change was calculated using the difference and percentage relative to the frequency under an axial load of 100 N at each stage of the bone healing pattern. A paired *t*-test was used to analyze the data with IBM SPSS Statistics version 29 software. A P-value < 0.05 was deemed statistically significant.

Results

This study analyzed twenty cadaveric tibial bones with five bone healing patterns. Each pattern was tested with four tibial bones. The frequency of each sample at each stage of bone healing under axial loads of 100, 200, 300, and 400 N, along with the difference in frequency between the 100 and 400 N axial loads, is presented in **Table 1**.

Table 1. Frequency data of cadaveric tibial samples at each stage of the bone healing pattern.

Sample no.	Bone healing pattern	Stage	Frequency (Hz)				Δ 100 N & 400 N (Hz, %)
			100 N	200 N	300 N	400 N	
1.	Gap distance	gap 10 mm	2397	2867	3368	3667	1270, 53.0%
		gap 7.5 mm	2490	2679	3395	3495	1005, 40.4%
		gap 5 mm	2434	2698	3026	3325	891, 36.6%
		gap 2.5 mm	2453	2693	2781	2863	410, 16.7%
		Heal	2321	2315	2316	2312	-9, -0.4%
2.	Gap distance	gap 10 mm	2396	2870	3347	3543	1147, 47.9%
		gap 7.5 mm	2517	2700	3185	3487	970, 38.5%
		gap 5 mm	2381	2734	3058	3214	833, 35.0%
		gap 2.5 mm	2458	2719	2798	2894	436, 17.7%
		Heal	2316	2312	2311	2314	-2, -0.1%
3.	Gap distance	gap 10 mm	2674	2845	3074	3421	747, 27.9%
		gap 7.5 mm	2567	2640	2889	3128	561, 21.9%
		gap 5 mm	2717	2844	2876	2987	270, 9.9%
		gap 2.5 mm	2733	2876	2905	2931	238, 8.7%
		Heal	2472	2466	2496	2473	1, 0.1%
4.	Gap distance	gap 10 mm	2661	2911	3001	3464	803, 30.2%
		gap 7.5 mm	2605	2701	2802	3306	701, 26.9%
		gap 5 mm	2807	2862	2884	3128	321, 11.4%
		gap 2.5 mm	2731	2883	2920	2964	233, 8.5%
		Heal	2447	2451	2489	2468	21, 0.9%
5.	Material replacement	Fracture	2657	2866	3151	3563	906, 34.1%
		Foam	2589	2816	3092	3282	693, 26.8%
		Rubber	2517	2616	2887	3055	538, 21.4%
		Saw bone	2520	2693	2747	2798	278, 11.0%
		Heal	2438	2447	2456	2481	43, 1.2 %
6.	Material replacement	Fracture	2701	2928	3270	3582	881, 32.6%
		Foam	2609	2845	3144	3263	654, 25.1%
		Rubber	2583	2676	2902	2998	415, 16.1%
		Saw bone	2476	2579	2745	2855	379, 15.3%
		Heal	2438	2447	2456	2481	43, 1.8%
7.	Material replacement	Fracture	2547	2747	3130	3394	847, 33.3%
		Foam	2579	2777	3057	3234	655, 25.4 %
		Rubber	2547	2724	2955	3109	562, 22.1%
		Saw bone	2492	2616	2662	2731	239, 9.6%
		Heal	2466	2401	2377	2377	-89, -3.6%
8.	Material replacement	Fracture	2610	2745	3113	3381	771, 29.5%
		Foam	2534	2737	3022	3194	660, 26.0%
		Rubber	2521	2592	2848	2984	463, 18.4%
		Saw bone	2462	2497	2622	2659	197, 8.0%
		Heal	2477	2471	2466	2484	7, 0.3%
9.	Healing from the outer side	Fracture	2520	2893	3047	3298	778, 30.9%
		Heal 25.0%	2475	2521	2535	2543	68, 2.8%
		Heal 50.0%	2494	2502	2525	2537	43, 1.7%
		Heal 75.0%	2519	2537	2542	2559	40, 1.6%
		Heal	2538	2547	2556	2581	43, 1.7%

Table 1. (Cont.) Frequency data of cadaveric tibial samples at each stage of the bone healing pattern.

Sample no.	Bone healing pattern	Stage	Frequency (Hz)				Δ 100 N & 400 N (Hz, %)
			100 N	200 N	300 N	400 N	
10.	Healing from the outer side	Fracture	2683	2876	3102	3498	815, 30.4%
		Heal 25.0%	2692	2708	2729	2743	51, 1.9%
		Heal 50.0%	2686	2711	2726	2737	51, 1.9%
		Heal 75.0%	2710	2731	2732	2759	49, 1.8%
		Heal	2722	2732	2766	2781	59, 2.2%
11.	Healing from the outer side	Fracture	2683	2727	3202	3534	851, 31.7%
		Heal 25.0%	2657	2727	2816	2884	227, 8.5%
		Heal 50.0%	2666	2640	2816	2809	143, 5.4%
		Heal 75.0%	2697	2640	2816	2802	105, 3.9%
		Heal	2683	2727	2746	2754	71, 2.7%
12.	Healing from the outer side	Fracture	2557	2683	3206	3534	977, 38.2%
		Heal 25.0%	2719	2721	2771	2909	190, 7.0%
		Heal 50.0%	2697	2640	2771	2909	212, 7.9%
		Heal 75.0%	2692	2700	2895	2862	170, 6.3%
		Heal	2727	2727	2727	2894	167, 6.1%
13.	Healing from the inner side	Fracture	2497	3034	3468	3419	922, 36.9%
		Heal 25.0%	2455	2506	2509	2519	64, 2.6%
		Heal 50.0%	2455	2455	2489	2512	57, 2.3%
		Heal 75%	2446	2506	2506	2506	60, 2.5%
		Heal	2466	2454	2450	2502	36, 1.5%
14.	Healing from the inner side	Fracture	2499	3104	3368	3406	907, 36.3%
		Heal 25.0%	2504	2506	2506	2544	40, 1.6%
		Heal 50.0%	2455	2455	2484	2500	45, 1.8%
		Heal 75.0%	2435	2506	2506	2518	83, 3.4%
		Heal	2411	2407	2455	2474	63, 2.6%
15.	Healing from the inner side	Fracture	2434	2909	3206	3534	1110, 45.2%
		Heal 25.0%	2545	2482	2557	2763	218, 8.6%
		Heal 50.0%	2557	2595	2634	2714	157, 6.1%
		Heal 75.0%	2505	2505	2557	2574	69, 2.8%
		Heal	2375	2474	2474	2434	59, 2.5%
16.	Healing from the inner side	Fracture	2434	2739	3206	3428	994, 40.8%
		Heal 25.0%	2482	2382	2457	2663	181, 7.3%
		Heal 50.0%	2419	2495	2534	2614	195, 8.1%
		Heal 75.0%	2376	2386	2364	2378	2, 0.1%
		Heal	2343	2349	2337	2337	3, 0.1%
17.	Healing from the middle	Fracture	2642	3266	3512	3581	939, 35.5%
		Heal 25.0%	2447	2446	2479	2482	35, 1.4%
		Heal 50.0%	2429	2440	2444	2454	25, 1.0%
		Heal 75.0%	2552	2526	2516	2557	5, 0.2%
		Heal	2516	2551	2527	2527	11, 0.4%
18.	Healing from the middle	Fracture	2610	3145	3426	3478	868, 33.3%
		Heal 25%	2579	2594	2624	2662	83, 3.2%
		Heal 50%	2534	2554	2583	2604	70, 2.8%
		Heal 75%	2515	2508	2498	2557	42, 1.7%
		Heal	2521	2521	2516	2527	6, 0.3%

Table 1. (Cont.) Frequency data of cadaveric tibial samples at each stage of the bone healing pattern.

Sample no.	Bone healing pattern	Stage	Frequency (Hz)				Δ 100 N & 400 N (Hz, %)
			100 N	200 N	300 N	400 N	
19.	Healing from the middle	Fracture	2509	2814	3209	3534	1025, 40.1%
		Heal 25%	2582	2619	2657	2752	170, 6.6%
		Heal 50.0%	2401	2497	2540	2540	139, 5.8%
		Heal 75.0%	2395	2474	2474	2514	119, 5.0%
		Heal	2456	2465	2514	2478	22, 0.9%
20.	Healing from the middle	Fracture	2473	2866	3209	3445	972, 39.3%
		Heal 25.0%	2545	2545	2582	2752	207, 8.1%
		Heal 50.0%	2449	2514	2597	2640	191, 7.8%
		Heal 75.0%	2395	2434	2474	2514	119, 5.0%
		Heal	2445	2458	2479	2478	33, 1.4%

Table 2. Mean frequency data of axial loading force in each stage of bone healing pattern.

Bone healing pattern	Stage	Mean of frequency (Hz)				*P*-value		
		100 N	200 N	300 N	400 N	100 N & 200 N	100 N & 300 N	100 N & 400 N
Gap distance	gap 10 mm	2532	2873	3198	3524	0.005*	0.002*	< 0.001*
	gap 7.5 mm	2545	2680	3068	3354	0.004*	0.01*	0.002*
	gap 5 mm	2585	2785	2961	3164	0.12	0.02*	0.005*
	gap 2.5 mm	2594	2793	2851	2913	0.08	0.03*	0.02*
	Heal	2389	2386	2403	2392	0.96	0.84	0.97
Material replacement	Fracture	2629	2822	3166	3480	0.01*	< 0.001*	< 0.001*
	Foam	2578	2794	3079	3243	0.0003*	< 0.001*	< 0.001*
	Rubber	2542	2652	2898	3037	0.02*	< 0.001*	< 0.001*
	Saw bone	2488	2596	2694	2761	0.04*	0.001*	0.005*
	Heal	2455	2442	2439	2456	0.48	0.51	0.97
Healing from the outer side	Fracture	2611	2795	3139	3466	0.03*	< 0.001*	< 0.001*
	Heal 25.0%	2636	2669	2713	2770	0.67	0.39	0.24
	Heal 50.0%	2636	2623	2710	2748	0.85	0.39	0.28
	Heal 75.0%	2655	2652	2746	2746	0.97	0.34	0.30
	Heal	2668	2683	2699	2753	0.81	0.65	0.33
Healing from the inner side	Fracture	2466	2947	3312	3447	0.001*	< 0.001*	< 0.001*
	Heal 25.0%	2497	2469	2507	2622	0.46	0.71	0.11
	Heal 50.0%	2472	2500	2535	2585	0.55	0.21	0.11
	Heal 75.0%	2441	2476	2483	2494	0.41	0.42	0.32
	Heal	2397	2421	2429	2437	0.56	0.47	0.41
Healing from the middle	Fracture	2559	3023	3339	3510	0.01*	< 0.001*	< 0.001*
	Heal 25.0%	2538	2551	2586	2662	0.81	0.38	0.15
	Heal 50.0%	2453	2501	2541	2560	0.24	0.10	0.08
	Heal 75.0%	2464	2486	2491	2536	0.66	0.55	0.18
	Heal	2485	2499	2509	2503	0.65	0.32	0.49

*Significant difference; $P < 0.05$.

Comparison of the mean frequencies among the axial loads of 200, 300, and 400 N with that of 100 N revealed significant differences in the fracture stage of all bone healing patterns. However, when comparing the axial loads of 100 and 400 N, only the gap distance and material replacement pattern exhibited notable findings in all stages, except for the healing stage. In all bone healing patterns, the healing stages exhibited no significant differences when comparing the frequencies under axial loads of 100, 200, 300, and 400 N. The data are presented in **Table 2**, and the graphs are shown in **Figure 5**.

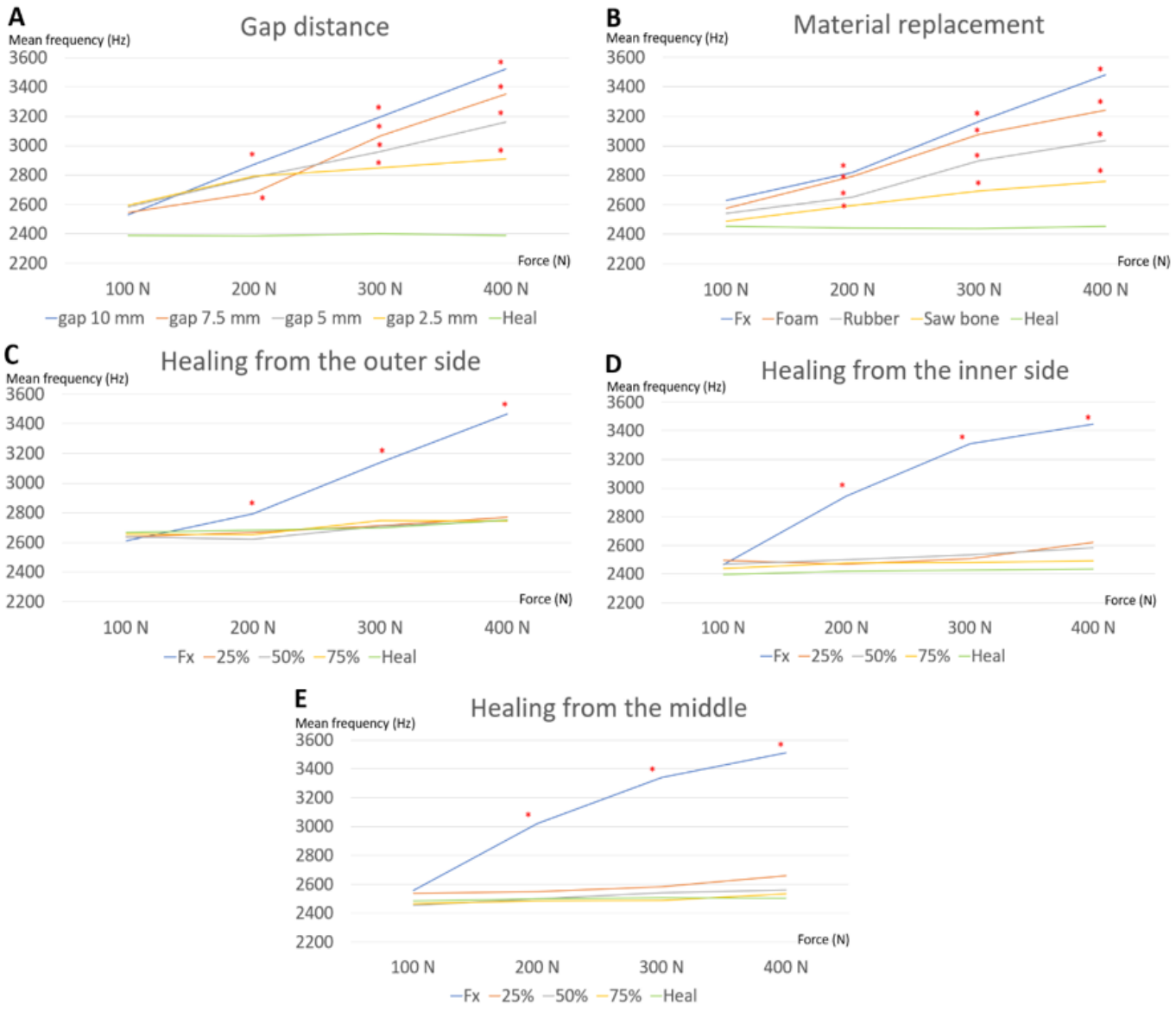

Figure 5. The graph illustrates the mean frequency of each stage under axial loads of 100 N, 200 N, 300 N, and 400 N for each bone healing pattern: **(A)** gap distance; **(B)** material replacement; **(C)** healing from the outer side; **(D)** healing from the inner side; **(E)** healing from the middle

Differences in the mean frequency between axial loads of 100 and 400 N at various fracture stages were 991.8 Hz (39.2%), 851.2 Hz (32.4%), 855.2 Hz (32.8%), 980.8 Hz (39.8%), and 951.0 Hz (37.2%) for gap distance, material replacement, and healing from the outer side, inner side, and middle, respectively. There were significant differences in all the bone healing patterns ($P = 0.004$, < 0.001, < 0.001, < 0.001, and < 0.001, respectively). In the healing stage of all the bone healing patterns, these differences were not statistically significant (2.8 Hz, $P = 0.70$; 1 Hz, $P = 0.98$; 85 Hz, $P = 0.06$; 40.3 Hz, $P = 0.06$; 18.0 Hz, $P = 0.06$, respectively). Only the differences of all stages of gap distance and material replacement patterns were significant, revealing gradual improvement (in the gap distance pattern: 10 mm 39.2% ($P = 0.004$); 7.5 mm 31.8% ($P = 0.005$); 5 mm 22.4% ($P = 0.04$); and 2.5 mm 12.3% ($P = 0.01$); for the material replacement pattern: the fracture was 32.4% ($P < 0.001$); foam 25.8% ($P < 0.001$); rubber 19.5% ($P = 0.001$); and saw bone 11.0% ($P = 0.006$)). The data are presented in **Table 3**, and the graphs are shown in **Figure 6**.

Table 3. The difference in mean frequency between an axial load of 100 N and 400 N at each stage of the bone healing pattern.

Bone healing pattern	Stage	Δ 100 N & 400 N	
		Hz, (%)	*P*-value
Gap distance	gap 10 mm	991.8, 39.2%	0.004*
	gap 7.5 mm	809.2, 31.8%	0.005*
	gap 5 mm	578.7, 22.4%	0.04*
	gap 2.5 mm	319.2, 12.3%	0.01*
	Heal	2.8, 0.1%	0.70
Material replacement	Fracture	851.2, 32.4%	< 0.001*
	Foam	665.5, 25.8%	< 0.001*
	Rubber	494.5, 19.5%	0.001*
	Saw bone	273.3, 11.0%	0.006*
	Heal	1, 0.0%	0.98
Healing from the outer side	Fracture	855.2, 32.8%	< 0.001*
	Heal 25.0%	134.0, 5.1%	0.06
	Heal 50.0%	112.2, 4.3%	0.07
	Heal 75.0%	91.0, 3.4%	0.06
	Heal	85.0, 3.2%	0.06
Healing from the inner side	Fracture	980.8, 39.8%	< 0.001*
	Heal 25.0%	125.8, 5.0%	0.06
	Heal 50.0%	113.5, 4.6%	0.06
	Heal 75.0%	53.5, 2.2%	0.06
	Heal	40.3, 1.7%	0.06
Healing from the middle	Fracture	951.0, 37.2%	< 0.001*
	Heal 25.0%	123.7, 4.9%	0.052
	Heal 50.0%	106.2, 4.3%	0.06
	Heal 75.0%	71.2, 2.9%	0.09
	Heal	18.0, 0.7%	0.06

**Significant difference, $P < 0.05$.

Discussion

To our knowledge, this study is the first to investigate which bone healing pattern is most suitable for detecting strain in any experiment. Moreover, this study comprehensively analyzes five stages of each bone healing pattern to evaluate the bone healing process in detail. Thus, this study evaluates the progression of bone healing, not only the fracture and bone union, and also determines the most suitable bone healing pattern for assessing bone healing. The strain change detection in this study employs a BUDWF plate[25] to identify frequency changes. In that experiment, a gap distance pattern is employed to evaluate the efficacy of bone healing assessment with a sawbone.

Numerous previous studies have examined devices that assess bone healing via strain changes using various methods, such as strain gauges,[16] changes in RRF,[17] wavelength,[18] piezoelectric voltage,[19] telemetry values,[20] tungsten displacement,[21] contrast media,[22] fluid levels,[23] force sensor,[24] and the frequency of wire in a BUDWF plate.[25] However, the standard bone healing pattern for assessment is yet to be established. Our results indicate that gap distance and material replacement pattern are the most suitable parameters for assessing bone healing through strain changes. The graphical abstract, including background, objective, material, methods, and results, is presented in **Figure 7.**

Most studies use the gap distance pattern with a fracture gap of 1 cm for experiments.[16-18, 21, 22, 25] This is because a larger gap distance is more sensitive in detecting strain changes. Furthermore, this study confirmed that a fracture gap of 1 cm was more effective in detecting strain changes through frequency changes compared to fracture gaps of 2.5, 5, and 7.5 mm under the same axial load. Although the 2.5 mm fracture gap exhibited the smallest difference in frequency change, it still significantly affected the frequency when comparing axial loads of 100 and 400 N.

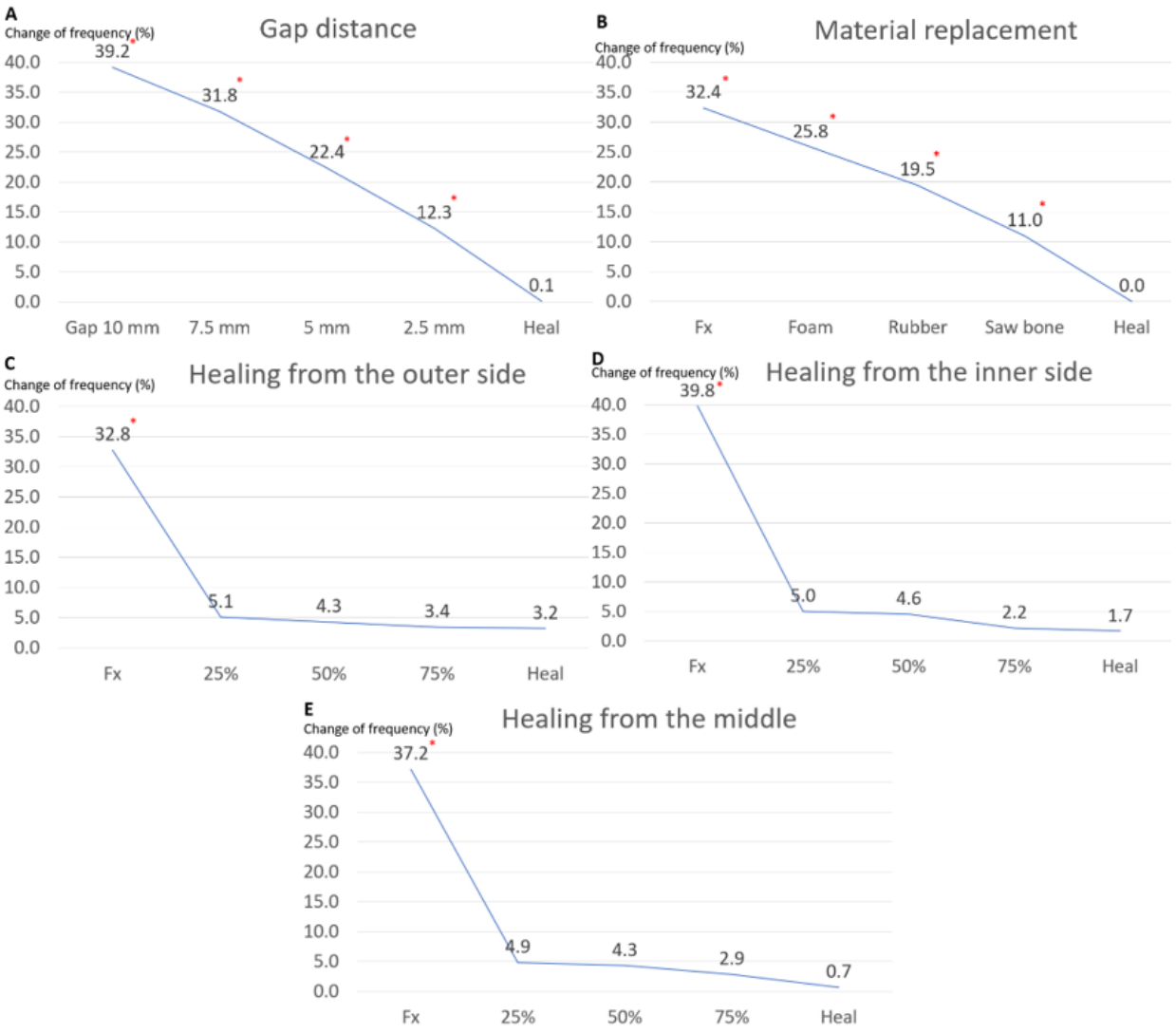

Figure 6. The graph illustrates the differences in mean frequency between an axial load of 100 N and 400 N at various fracture stages for each bone healing pattern: **(A)** gap distance; **(B)** material replacement; **(C)** healing from the outer side; **(D)** healing from the inner side; **(E)** healing from the middle.

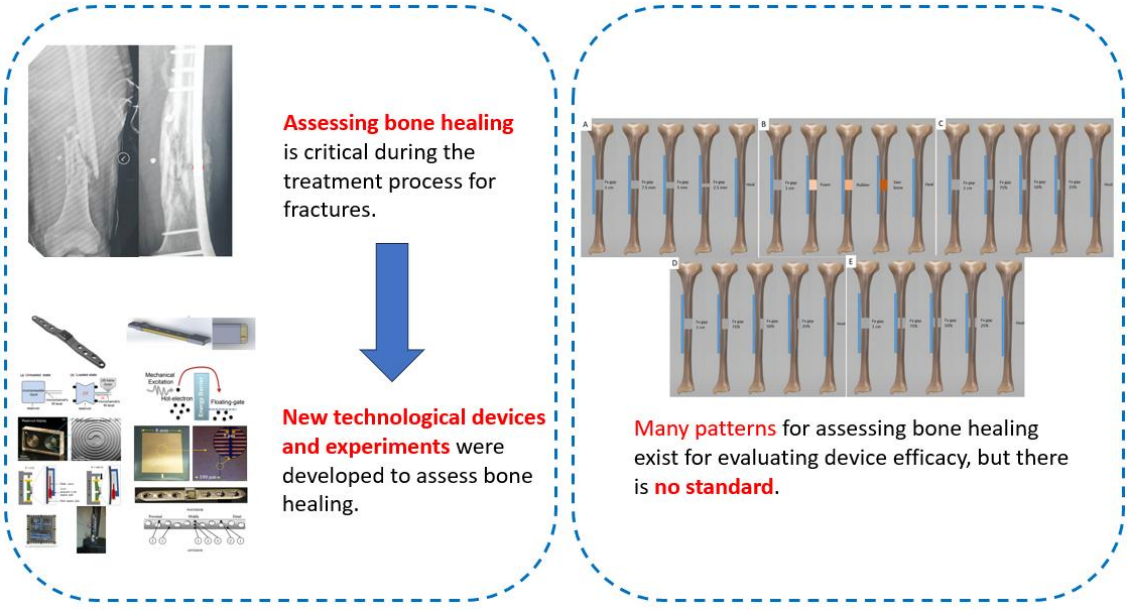

Figure 7. The picture illustrates the graphical abstract of this study.

The material replacement pattern is also popular in many studies.[19-24] The materials chosen to represent bone healing as soft or hard callus depend on the elastic modulus of the material. In previous studies, silicone or polymer foam was used to represent soft callus, while PMMA, wood, or acrylic was used to represent hard callus. In this study, foam, rubber, and sawbone were used to represent the bone healing process with an increasing elastic modulus that mimics real bone as closely as possible. The results revealed a gradual frequency change that was related to the elastic modulus of the material replacements. The minimum frequency change between the axial loads of 100 and 400 N was found in the bone healing group, with gradual differences in sawbone, rubber, and foam (0.0%, 11.0%, 19.5%, and 25.8%, respectively).

The healing process from the outer side, inner side, and middle exhibited significantly different frequency changes under axial loads of 100 and 400 N only during the fracture stage. This is because if the bone experiences a fracture with a bone bridge, even at 25.0%, it affects the evaluation of strain changes. The axial force in a bone fracture without a bone bridge transfers directly to the plate, thereby causing high strain and high frequency. However, when a bone bridge occurs, even if only 25.0%, the axial force transmits through the bone and plate, thereby increasing the second moment of area. This makes it harder to bend the plate and thus more difficult to alter the strain of the plate. The axial force is transmitted through the bone and plate, which results in minimal change in the strain on the plate.

Although this study focused on the bone healing pattern, the results demonstrated the effectiveness of the BUDWF plate in assessing bone healing. This supports the findings of Chancharoen P, *et al.,*[25] who stated that detecting changes in the wire frequency on the plate could assess bone healing and help identify bone union or nonunion. This could be beneficial in real-world situations. However, this plate was still a prototype and requires further experimental validation, especially in real environments surrounded by soft tissue and fluid that may affect wire frequency changes.

This study had a few limitations. First, it was a cadaveric study that did not accurately assess real bone healing, which may have factors that influenced the evaluation. However, this study tested five different bone healing patterns to evaluate and explore the five stages of each healing pattern, thereby creating a situation that mimics the real bone healing process as closely as possible. Second, there was a limited number of cadaveric bones included in each bone healing pattern. However, the results revealed the same trend for all samples in each group. Third, this study applied an axial load of 400 N (which is half the weight of an 80 kg human body). The results may change if the axial load increases, but we selected 400 N to resemble partial weight bearing, which correlates with the postoperative rehabilitation protocol for patients with a midshaft tibial fracture that is treated with plate fixation.

Conclusion

The pattern of bone healing influences the assessment of bone union by detecting changes in strain. Methods that involve gap distance and material replacement are the most suitable for mimicking the process of normal bone healing, which demonstrates a gradual process of bone healing by decreasing the bone gap and filling it with representative bone callus material. The bone healing pattern from the outer side, inner side, and middle is not appropriate to use because of the lack of gradual changes in bone healing. Although this study is a cadaveric experiment, the authors hope that this study will serve as a reference for future research that explores new devices or methods to evaluate bone healing initially in cadavers and then for application in humans.

Author contributions

CA, CV, and PT contributed substantially to the concept and design of this study, acquiring the data, reviewing the literature, and its analysis and interpretation. CA, PC, and ST contributed substantially to acquiring the data. CA contributed to drafting the manuscript. CA, CV, and PT edited the manuscript critically for important intellectual content. All authors approved the final version submitted for publication and accept responsibility for statements made in the published article.

Acknowledgments

The authors would like to express their gratitude to all participants who were involved in this study.

Conflict of interest statement

Each author declares that there are no commercial associations (consultancies, stock ownership, equity interest, patent/licensing arrangements, etc.) that might pose a conflict of interest in connection with the submitted article related to the author or any immediate family members.

Data sharing statement

The data supporting this study's findings are available from the corresponding author (P.T.) upon reasonable request.

ORCID

Chavarin Amarase https://orcid.org/0000-0001-5249-3781
Chanyaphan Virulsri https://orcid.org/0000-0002-1676-6970
Pairat Tangpornprasert https://orcid.org/0000-0002-2216-4976
Pisitpong Chancharoen https://orcid.org/0009-0001-5621-5874
Saran Tantavisut https://orcid.org/0000-0002-3767-4653

References

1. Zhu Z, Zhang T, Shen Y, Shan PF. The burden of fracture in China from 1990 to 2019. Arch Osteoporos 2023;19:1.
2. Nyrhi L, Kuitunen I, Ponkilainen V, Huttunen TT, Mattila VM. Incidence of fracture hospitalization and surgery during pregnancy in Finland-1998-2017: a retrospective register-based cohort study. Arch Orthop Trauma Surg 2023;143:5719–25.
3. GBD 2019 Fracture Collaborator. Global, regional, and national burden of bone fractures in 204 countries and territories, 1990-2019: a systematic analysis from the Global Burden of Disease Study 2019. Lancet Healthy Longev 2021;2:e580–e92.
4. Wu CY, Lee HS, Tsai CF, Hsu YH, Yang HY. Secular trends in the incidence of fracture hospitalization between 2000 and 2015 among the middle-aged and elderly persons in Taiwan: A nationwide register-based cohort study. Bone 2022;154:116250.
5. Baertl S, Alt V, Rupp M. Surgical enhancement of fracture healing - operative vs. nonoperative treatment. Injury 2021;52 Suppl 2:S12–S7.
6. Nicholson JA, Makaram N, Simpson A, Keating JF. Fracture nonunion in long bones: a literature review of risk factors and surgical management. Injury. 2021;52 Suppl 2:S3–S11.
7. Siverino C, Metsemakers WJ, Sutter R, Della Bella E, Morgenstern M, Barcik J, et al. Clinical management and innovation in fracture non-union. Expert Opin Biol Ther 2024;24:973–91.
8. Nicholson JA, Yapp LZ, Keating JF, Simpson A. Monitoring of fracture healing. Update on current and future imaging modalities to predict union. Injury 2021;52 Suppl 2:S29–S34.
9. Cunningham BP, Brazina S, Morshed S, Miclau T 3rd. Fracture healing: A review of clinical, imaging and laboratory diagnostic options. Injury 2017;48 Suppl 1:S69–S75.
10. Craig JG, Jacobson JA, Moed BR. Ultrasound of fracture and bone healing. Radiol Clin North Am 1999;37:737–51.
11. Willems A, Içli C, Waarsing JH, Bierma-Zeinstra SMA, Meuffels DE. Bone union assessment with computed tomography (ct) and statistical associations with mechanical or histological testing: a systematic review of animal studies. Calcif Tissue Int 2022;110:147–61.
12. Schwarzenberg P, Darwiche S, Yoon RS, Dailey HL. Imaging modalities to assess fracture healing. Curr Osteoporos Rep 2020;18:169–79.
13. Haffner-Luntzer M, Müller-Graf F, Matthys R, Hägele Y, Fischer V, Jonas R, et al. Evaluation of high-resolution in vivo MRI for longitudinal analysis of endochondral fracture healing in mice. PLoS One 2017;12:e0174283.
14. Crönlein M, Rauscher I, Beer AJ, Schwaiger M, Schäffeler C, Beirer M, et al. Visualization of stress fractures of the foot using PET-MRI: a feasibility study. Eur J Med Res 2015;20:99.
15. Sollini M, Trenti N, Malagoli E, Catalano M, Di Mento L, Kirienko A, et al. [^{18}F]FDG PET/CT in non-union: improving the diagnostic performances by using both PET and CT criteria. Eur J Nucl Med Mol Imaging 2019; 46:1605–15.
16. Windolf M, Varjas V, Gehweiler D, Schwyn R, Arens D, Constant C, et al. Continuous implant load monitoring to assess bone healing status-evidence from animal testing. Medicina (Kaunas) 2022;58:858.
17. McGilvray KC, Unal E, Troyer KL, Santoni BG, Palmer RH, Easley JT, et al. Implantable microelectromechanical sensors for diagnostic monitoring and post-surgical prediction of bone fracture healing. J Orthop Res 2015;33:1439–46.
18. Najafzadeh A, Serandi Gunawardena D, Liu Z, Tran T, Tam HY, Fu J, et al. Application of fibre bragg grating sensors in strain monitoring and fracture recovery of human femur bone. Bioengineering (Basel) 2020;7:98.
19. Borchani W, Aono K, Lajnef N, Chakrabartty S. Monitoring of postoperative bone healing using smart trauma-fixation device with integrated self-powered piezo-floating-gate sensors. IEEE Trans Biomed Eng 2016;63:1463–72.
20. Kienast B, Kowald B, Seide K, Aljudaibi M, Faschingbauer M, Juergens C, et al. An electronically instrumented internal fixator for the assessment of bone healing. Bone Joint Res 2016;5:191–7.
21. Pelham H, Benza D, Millhouse PW, Carrington N, Arifuzzaman M, Behrend CJ, et al. Implantable strain sensor to monitor fracture healing with standard radiography. Sci Rep 2017;7:1489.

22. Rajamanthrilage A, Arifuzzaman M, Millhouse P, Pace T, Behrend C, DesJardins J, et al. Measuring orthopedic plate strain to track bone healing using a fluidic sensor read via plain radiography. IEEE Trans Biomed Eng 2022;69:278–85.
23. Umbrecht F, Wägli P, Dechand S, Gattiker F, Neuenschwander J, Sennhauser U, et al. Wireless implantable passive strain sensor: design, fabrication and characterization. J Micromech Microeng 2010; 20:085005.
24. Ledet EH, Caparaso SM, Stout M, Cole KP, Liddle B, Cady NC, et al. Smart fracture plate for quantifying fracture healing: preliminary efficacy in a biomechanical model. J Orthop Res 2022;40:2414–20.
25. Chancharoen P, Tangpornprasert P, Amarase C, Tantavisut S, Virulsri C. Design of osteosynthesis plate for detecting bone union using wire natural frequency. Sci Rep 2024;14:12569.
26. Leong PL, Morgan EF. Measurement of fracture callus material properties via nanoindentation. Acta Biomater 2008;4:1569–75.